Available online at www.sciencedirect.com
ScienceDirect
Journal of Sound and Vibration 320 (2009) 793–807
JOURNAL OF SOUND AND VIBRATION
www.elsevier.com/locate/jsvi

Identification of the bending stiffness matrix of symmetric laminates using regressive discrete Fourier series and finite differences

F.B. Batista*, E.L. Albuquerque, J.R.F. Arruda, M. Dias Jr.

Faculty of Mechanical Engineering, University of Campinas, Cidade Universitária Zeferino Vaz, 13083-970 Campinas, SP, Brazil

Received 30 August 2007; received in revised form 17 July 2008; accepted 26 August 2008
Handling Editor: S. Bolton
Available online 8 October 2008

Abstract

It is known that the elastic constants of composite materials can be identified by modal analysis and numerical methods. This approach is nondestructive, since it consists of simple tests and does not require high computational effort. It can be applied to isotropic, orthotropic, or anisotropic materials, making it a useful alternative for the characterization of composite materials. However, when elastic constants are bending constants, the method requires numerical spatial derivatives of experimental mode shapes. These derivatives are highly sensitive to noise. Previous works attempted to overcome the problem by using special optical devices. In this study, the elastic constant is identified using mode shapes obtained by standard laser vibrometers. To minimize errors, the mode shapes are first smoothed by regressive discrete Fourier series, after which their spatial derivatives are computed using finite differences. Numerical simulations using the finite element method and experimental results confirm the accuracy of the proposed method. The experimental examples reported here consist of an isotropic steel plate and an orthotropic carbon–epoxy plate excited with an electromechanical shaker. The forced response is measured at a large number of points, using a laser Doppler vibrometer. Both numerical and experimental results were satisfactory.

1. Introduction

Composite materials today are used in many engineering fields because they have particular properties and characteristics that other commonly used materials lack. In other words, unlike other structural materials, such as metals, ceramics or polymers, their properties are flexible and can be changed according to design requirements. Thanks to the numerous possible component combinations and arrangements, designers and engineers can meet the specific needs of a particular design. However, the anisotropic behavior of composite materials makes their structural analysis more complex. Their anisotropy increases the number of independent elastic properties, making it more difficult to identify and determine the values of these properties in

*Corresponding author. Tel.: +55 19 3521 3187; fax: +55 19 3289 3722.
E-mail addresses: fabianchi@fem.unicamp.br (F.B. Batista), ederlima@fem.unicamp.br (E.L. Albuquerque), arruda@fem.unicamp.br (J.R.F. Arruda), milton@fem.unicamp.br (M. Dias Jr.).

0022-460X/$ - see front matter
doi:10.1016/j.jsv.2008.08.030

Nomenclature

$\mathbf{A}$, $\mathbf{B}$	matrices
D_{ij}	bending stiffness constants
h	plate thickness
k, l, m, n	integer indices
M, N	data size, i.e., number of rows and columns, respectively
R, C	DFS period size, rows, and columns, respectively
p	frequency lines along the ξ direction
q	frequency lines along the η direction
S	plate domain
t	time
w	transverse deflection function of the plate
W_M,W_N	Mth and Nth root of unity, respectively
W_R, W_C	Rth and Cth root of unity, respectively
$\mathbf{W}_R$, $\mathbf{W}_C$	matrices of elements ${W_R}^{mk}$ and ${W_C}^{ln}$, respectively
x_{mn}	discretized data
$x^{(S)}$	smoothed discretized data
x, y	coordinates in the plane of the plate
X_{kl}	two-dimensional Euler–Fourier coefficients
$\boldsymbol{\varepsilon}$	error matrix
ξ, η	orthogonal directions in the two-dimensional domain
ρ	density of the plate material
Φ	transverse deflection amplitude function of the plate
ω	natural frequency

experimental tests. The elastic properties of composite materials can be characterized through dynamic or static tests, which are well known and have long been in use. However, despite the simplicity of static tests, they have disadvantages, e.g., the fact that they are destructive and require a number of samples with fiber orientations specified by standards [1]. The fiber orientation of samples seldom coincides with the fiber orientation specified in a design. Furthermore, some variables are difficult to control during tests and can contribute to scatter experimental results, e.g., nonuniform stress fields near the ends of a sample due to clamped boundary conditions. These aspects render static tests less attractive for composites. An alternative approach for determining elastic constants is to combine modal analysis and numerical methods. This type of approach allows for the identification of elastic constants using only one sample or even the real composite material. These elastic constants represent global values and therefore offer the advantage of being little influenced by local imperfections. In this type of test, samples are usually thin plates that reflect Kirchhoff's hypotheses, cylindrical shells, or beams. The modal analysis is required to supply the input data for the numerical methods that compute the elastic constants. Generally, the input data of numerical methods are natural frequencies and/or mode shapes. For numerical reasons, first modes associated to lower frequencies are preferred. Many authors have proposed calculating elastic constants by iterative procedures using the Rayleigh–Ritz method [2–6] and finite elements [7–12]. In these works, an objective function is created and minimized. The objective function is a function of the natural frequencies obtained numerically and experimentally. The main disadvantages of these iterative procedures are due to the dependency on the optimization method. An initial guess for elastic constants should be given and there is always the risk of stopping in a local minimum.

Grédiac and Paris [13] proposed an alternative approach that directly identifies the elastic parameters without using an iterative procedure. In this case, vibration amplitudes and frequencies are input data to solve a linear system based on the equation that governs the transversal vibrations of anisotropic thin plates under free response. However, because this method requires the computation of spatial derivatives of mode shapes, its results are strongly dependent on the noise level of the experimental mode shapes. Hence, it is very difficult to use this method with experimental data obtained from standard modal analysis procedures. The experimental noise level must be reduced in order to overcome difficulties in the numerical computation of spatial derivatives of the mode shapes. Grédiac et al. [14] suggested the use of special optical devices in modal tests. However, these devices are not common in most vibration labs.

In this paper, the regressive discrete Fourier series (RDFS) is applied to smooth mode shapes from both numerical and experimental tests, and consequently, to reduce noise. Elastic constants are then computed following the procedure proposed by Grédiac and Paris [13]. Second-order spatial partial derivatives of mode

shapes are computed by finite differences from the smoothed shapes. Numerical and experimental tests were carried out to assess the accuracy of the proposed method. It is shown that the method can compute the elastic constant accurately, even when the input data contains noise.

2. Numerical and theoretical procedures for the identification of elastic constants

2.1. Review of the method to compute bending stiffness

The method proposed by Grédiac and Paris [13] consists of obtaining elastic constants based on the partial differential equation that governs the transversal vibration of an anisotropic thin plate (Kirchhoff's plate). This equation is given by

$$D_{11}\frac{\partial^4 w}{\partial x^4}+4D_{16}\frac{\partial^4 w}{\partial x^3\partial y}+2(D_{12}+2D_{66})\frac{\partial^4 w}{\partial x^2\partial y^2}+4D_{26}\frac{\partial^4 w}{\partial x\partial y^3}+D_{22}\frac{\partial^4 w}{\partial y^4}=-\rho h\frac{\partial^2 w}{\partial t^2}, \tag{1}$$

where D_{ij} are thin plate bending stiffness constants, ρ is the mass density of the material, h is the plate thickness, x and y are coordinates of the plate, t is time, and $w(x,y,t)$ is the deflection function that represents the transversal displacement of a point of the plate at an instant t. Eq. (1) does not state the global equilibrium of the plate since the excitation force and damping are not considered. However, for many composite materials as, for example, aeronautic carbon–epoxy tested in this work, the damping is low enough to disregard its contribution in the formulation. Besides, if the input data refer to resonant response of the plate, the work provided by the excitation is balanced by internal dissipation of the plate. A detailed discussion about when excitation and damping should be considered in Eq. (1) can be found in Giraudeau and Pierron [15].

After some mathematical manipulations of Eq. (1), Grédiac and Paris [13] obtained a linear system in which the unknown variables are the elastic constants. Briefly, the sequence of operations is as follows: (a) multiply both sides of Eq. (1) by an arbitrary weighting function; (b) integrate twice by parts along the plate domain; (c) eliminate the boundary integrals by applying the free–free boundary conditions; (d) decompose the displacement function $w(x,y,t)$ as a product of the deflection amplitude $\Phi(x,y)$ and $\sin(\omega t)$, where ω is the natural frequency of a particular mode shape of the plate; and (e) choose appropriate weighting functions and mode shapes to build the matrix of the linear system. At this point, as Grédiac and Paris [13] explain, the choice of mode shapes associated with the weighting function is extremely important for the accuracy of this method. Three particular modes are strongly dependent on the required coefficients D_{ij}: a twisting mode that strongly depends on terms D_{66}, D_{16}, and D_{26}; a bending mode along direction 1 that strongly depends on terms D_{11}, D_{12}, and D_{16}, and a bending mode along direction 2 that strongly depends on D_{22}, D_{12}, and D_{26}. These modes present smooth curvatures and are generally among the first modes, with lower frequencies. If these modes are not found, it is recommended to use modes that have shapes similar to theirs. Furthermore, they are modes that can be approximated by quadratic functions with constant curvatures: x^2, y^2, and xy. For this reason, these quadratic functions were the weighting functions chosen by Grédiac and Paris [13]. Thus, using these previous quadratic-weighting functions, the following simplified system of equations can be obtained:

$$\begin{bmatrix}
\cdots & \cdots & \cdots & \cdots & \cdots & \cdots \\
K_{xx}^{(j)} & 0 & K_{yy}^{(j)} & 0 & K_{xy}^{(j)} & 0 \\
0 & K_{yy}^{(j)} & K_{xx}^{(j)} & 0 & 0 & K_{xy}^{(j)} \\
0 & 0 & 0 & K_{xy}^{(j)} & K_{xx}^{(j)} & K_{yy}^{(j)} \\
\cdots & \cdots & \cdots & \cdots & \cdots & \cdots \\
K_{xx}^{(k)} & 0 & K_{yy}^{(k)} & 0 & K_{xy}^{(k)} & 0 \\
0 & K_{yy}^{(k)} & K_{xx}^{(k)} & 0 & 0 & K_{xy}^{(k)} \\
0 & 0 & 0 & K_{xy}^{(k)} & K_{xx}^{(k)} & K_{yy}^{(k)} \\
\cdots & \cdots & \cdots & \cdots & \cdots & \cdots
\end{bmatrix}
\begin{Bmatrix} D_{11} \\ D_{22} \\ D_{12} \\ D_{66} \\ D_{16} \\ D_{26} \end{Bmatrix}
=-\frac{\rho h}{2}
\begin{Bmatrix}
\cdots \\
\omega_j^2\int_S \Phi^{(j)}x^2\,\mathrm{d}S \\
\omega_j^2\int_S \Phi^{(j)}y^2\,\mathrm{d}S \\
\omega_j^2\int_S \Phi^{(j)}xy\,\mathrm{d}S \\
\cdots \\
\omega_k^2\int_S \Phi^{(k)}x^2\,\mathrm{d}S \\
\omega_k^2\int_S \Phi^{(k)}y^2\,\mathrm{d}S \\
\omega_k^2\int_S \Phi^{(k)}xy\,\mathrm{d}S \\
\cdots
\end{Bmatrix}, \tag{2}$$

where indices j and k each represent a specific mode shape and S is the plate domain. Elements of the matrix of Eq. (2) are given by

$$K_{xx} = \int_S \frac{\partial^2 \Phi(x,y)}{\partial x^2} \mathrm{d}S, \quad K_{yy} = \int_S \frac{\partial^2 \Phi(x,y)}{\partial y^2} \mathrm{d}S, \quad K_{xy} = \int_S \frac{\partial^2 \Phi(x,y)}{\partial x \partial y} \mathrm{d}S. \tag{3}$$

Eq. (2) can be represented in matrix form as

$$\mathbf{AD} = \mathbf{B}, \tag{4}$$

where, considering L as the number of modes used in the linear system of equations, $\mathbf{A}$ is a $3L \times 6$ matrix, $\mathbf{D}$ is a 6×1 matrix, and $\mathbf{B}$ is a $3L \times 1$ matrix. As can be seen, Eq. (4) is an overdetermined system of equations. The solution can be found by least squares:

$$\mathbf{D} = (\mathbf{A}^{\mathrm{T}}\mathbf{A})^{-1}(\mathbf{A}^{\mathrm{T}}\mathbf{B}). \tag{5}$$

Because finite differences are quite sensitive to noise, this method is not suitable for computing derivatives of experimental mode shapes that contain noise. This work proposes the use of the RDFS to smooth the data before computing the numerical derivatives by finite differences.

2.2. The regressive discrete Fourier series

It is known that signal derivatives are extremely sensitive to noise. This can be explained by the fact that the amplitude of the derivative of a sine wave is proportional to its frequency. Thus, the noise derivative becomes predominant for a low frequency signal, even at very low noise levels, due to the high frequency content of the noise. That is why finite difference schemes are not suitable for differentiating noise-contaminated signals [6]. Smoothing techniques can be used in experimental modal analysis applications to smooth spatially dense measured operating shapes. In this work is used a smoothing technique proposed by Arruda [16] called RDFS. It uses least squares to estimate the coefficients of a two-dimensional discrete Fourier series with arbitrary periods and arbitrary frequency resolutions. This formulation can be used for rectangular or arbitrary-shaped domains, as shown by Arruda [16]. Unlike the discrete Fourier transform, one uses approximation instead of interpolation, which decreases the effect of periodization, i.e., the leakage. Unlike the discrete Fourier series, the original length of the data is not assumed to be equal to the period, and the number of line frequencies is not assumed to be equal to the size of the data. The RDFS is expressed as

$$x_{mn}(\xi,\eta) = \sum_{k=-p}^{p} \sum_{l=-q}^{q} X_{kl} W_R^{mk} W_C^{ln} + \varepsilon_{mn}; \quad m = 0,\ldots,M-1; \;\; n = 0,\ldots,N-1, \tag{6}$$

where ξ and η are orthogonal directions in the two-dimensional domain, x_{mn} is the discretized data with constant resolution $\Delta\xi$ and $\Delta\eta$, k, l, m, and n are integer indices, M and N are the data size, i.e., number of rows and columns, respectively, R and C are the period size of the discrete Fourier series, rows and columns, respectively, $W_R = \exp(\mathrm{i}2\pi/R)$ and $W_C = \exp(\mathrm{i}2\pi/C)$ are the Rth and Cth roots of unity, respectively, X_{kl} are the two-dimensional Euler–Fourier coefficients, and ε_{mn} is the element of the error matrix $\boldsymbol{\varepsilon}$. The length of the data in the ξ direction is $M\Delta\xi$, but the period of the discrete Fourier series is $R > M$. The number of frequency lines kept when filtering is $p \ll M$. In the same way, the length of the data in the η direction is $N\Delta\eta$, but the period of the discrete Fourier series is $C > N$. The number of frequency lines kept when filtering is $q \ll N$. Thus, an approximation of x_{mn} is made and the Euler–Fourier coefficients cannot be calculated by the discrete Fourier transform. Rewriting Eq. (6) in a matrix form, one has

$$\mathbf{x} = \mathbf{W}_R \mathbf{X} \mathbf{W}_C + \boldsymbol{\varepsilon}, \tag{7}$$

where $\boldsymbol{\varepsilon}$ is error vector in arbitrary domain RDFS.

The least-square solution is given by

$$\mathbf{X} = (\mathbf{W}_R^H \mathbf{W}_R)^{-1} \mathbf{W}_R^H \mathbf{x} \mathbf{W}_C^H (\mathbf{W}_C \mathbf{W}_C^H)^{-1}. \tag{8}$$

The superscript H denotes the complex conjugate transpose of a matrix. It should be noted that matrices to be inverted have a very small size, i.e. $(2p+1 \times 2p+1)$ and $(2q+1 \times 2q+1)$, respectively. The smoothed shape

is obtained from

$$\mathbf{x}^{(S)} = \mathbf{W}_R \mathbf{X} \mathbf{W}_C. \tag{9}$$

2.3. *The optimized* RDFS

It is possible to write the period of the discrete Fourier series as $R = K_\xi M$ along ξ direction and $C = K\eta N$ along η direction. In practice, ratios K_ξ and K_η are usually unknown and they should be estimated as well together with the residues leading to a nonlinear least-squares problem. An approach based on an RDFS and called optimized regressive discrete Fourier series (ORDFS) was introduced by Vanherzeele [17]. It allows both ratios K_ξ and K_η to be estimates using a more robust and computationally faster linear least-squares approach. Using the built-in function *lsqnonlin* of the Signal Processing Toolbox in Matlab, it is possible to estimate these unknown ratios together with the unknown coefficients $\mathbf{X}$ of Eq. (7) using a classical Gauss–Newton iterative procedure. For this optimization problem, the objective function represents the residue computed by nodal difference between the original signal (that in this work is the original mode shape in a specific frequency), having noise, and its respective filtered signal (smoothed or virtual mode shape in the same frequency). Ratios K_ξ and K_η are changed in each iterative minimization step and will be the global parameters for this step. After iterative process, the optimum values for these optimization variables K_ξ and K_η are used in the calculation of $\mathbf{x}^{(S)}$, or more specifically, for this work, in the calculation of the smoothed mode shape.

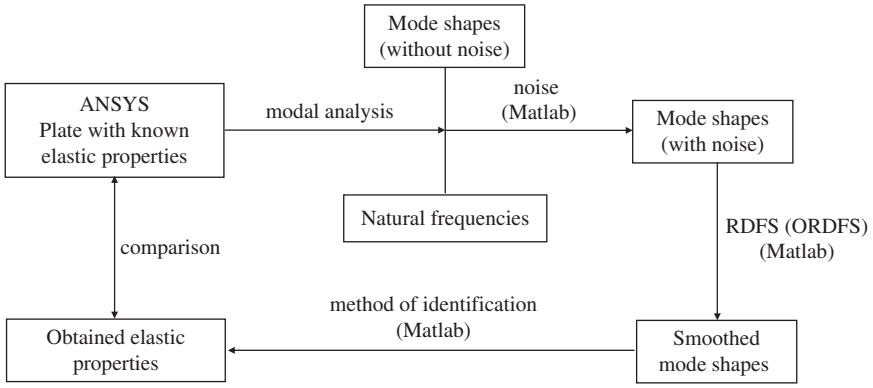

Fig. 1. Numerical identification process of the elastic properties.

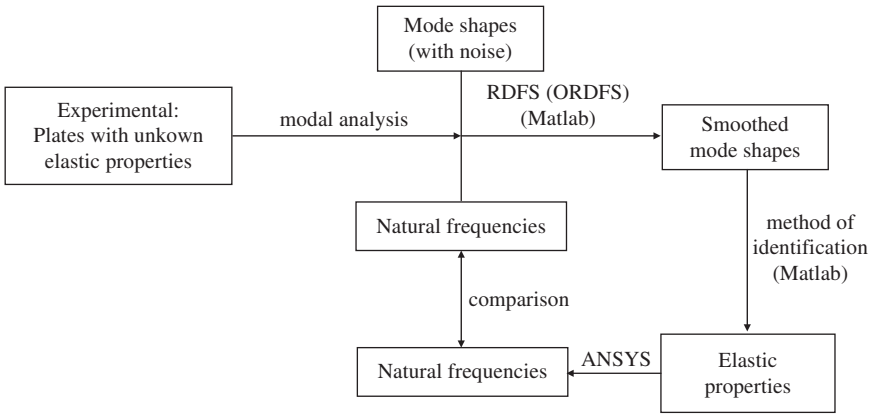

Fig. 2. Experimental identification process of the elastic properties.

Table 1
Properties and dimensions of the numerical plate used to assess the method

Characteristic of the anisotropic plate	
D_{11} (N mm)	64,363.9
D_{22} (N mm)	24,155.8
D_{12} (N mm)	8875.1
D_{66} (N mm)	10,032.7
D_{16} (N mm)	6019.6
D_{26} (N mm)	6019.6
Width (mm)	350
Length (mm)	450
Thickness of the laminate (mm)	2.1
Density (kg/mm^3)	1.510

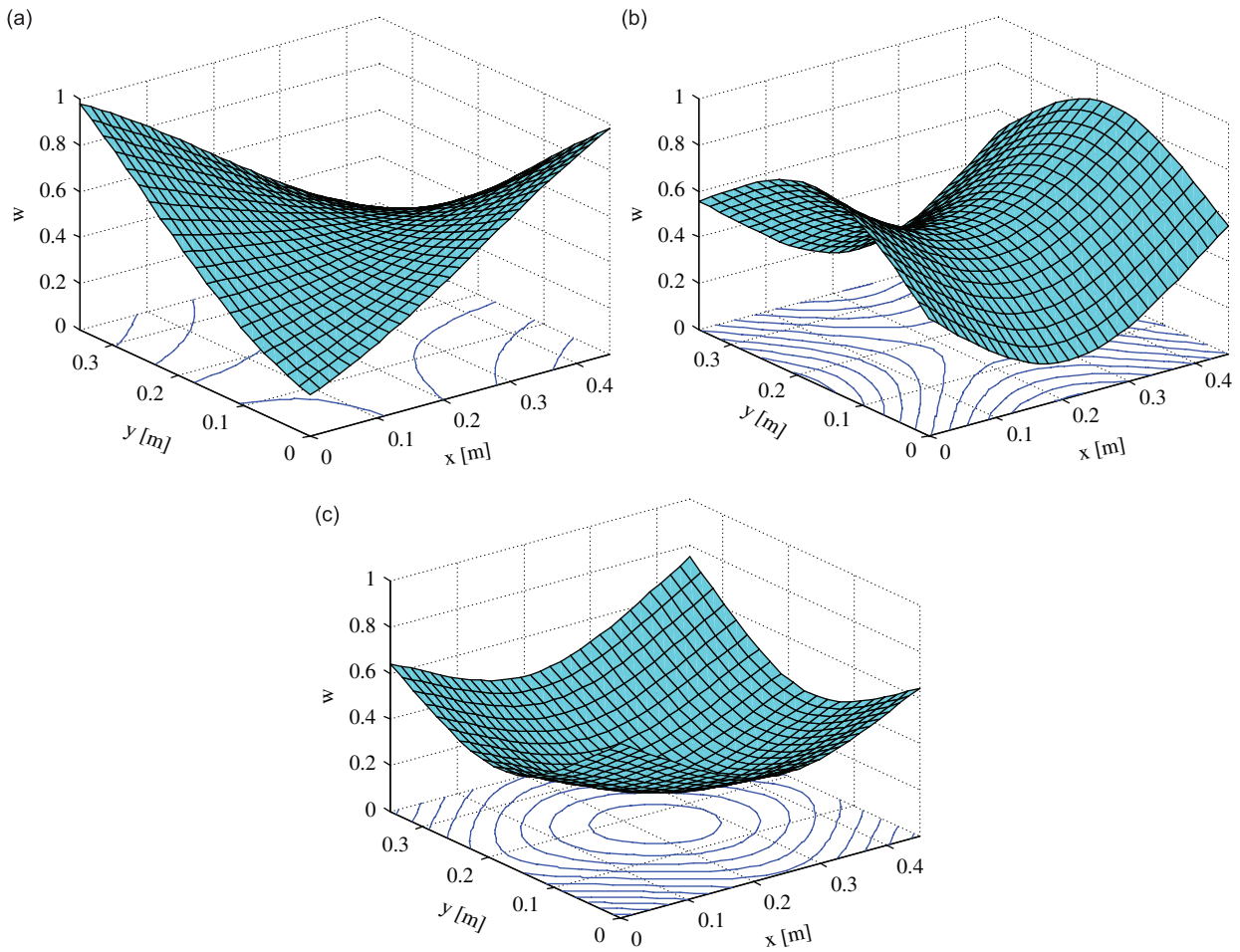

Fig. 3. Numerical modes obtained from ANSYS: (a) mode shape 1, (b) mode shape 2 and (c) mode shape 3.

3. Complete identification process

In this section, numerical and experimental analyses were carried out in order to verify the accuracy of the RDFS when used as smoothing method of the mode shape. The numerical mode shapes with their

corresponding natural frequencies were obtained by commercial finite element program (ANSYS 10.0), and noise was randomly generated on these modes (more details in Section 4). The experimental modal analysis was carried out using a laser Doppler vibrometer, as can be seen in Section 5. Two plates were tested: an isotropic steel plate and an orthotropic carbon/epoxy plate. Figs. 1 and 2 show, respectively, the numerical and experimental identification processes of elastic properties.

4. Numerical analysis

4.1. Presentation of the validation process

Initially, a hypothetical anisotropic plate was used to the numerical modal analysis. Its characteristics can be seen in Table 1. It was used a Pentium IV processor with 2.4 MHz of clock and 1 GBytes of RAM. The natural frequencies and mode shapes were computed using a mesh of 150 elements with eight nodes per element (ANSYS element SHELL93). The plate was considered under free-edge boundary conditions. In order to simulate noise, random numbers were added to the amplitude of the mode shapes. These random numbers have a maximum amplitude of 5%, 10%, or 15% of the maximum magnitude of the deflection. First and second derivatives were computed by finite differences with and without noise, using or not the smoothing process.

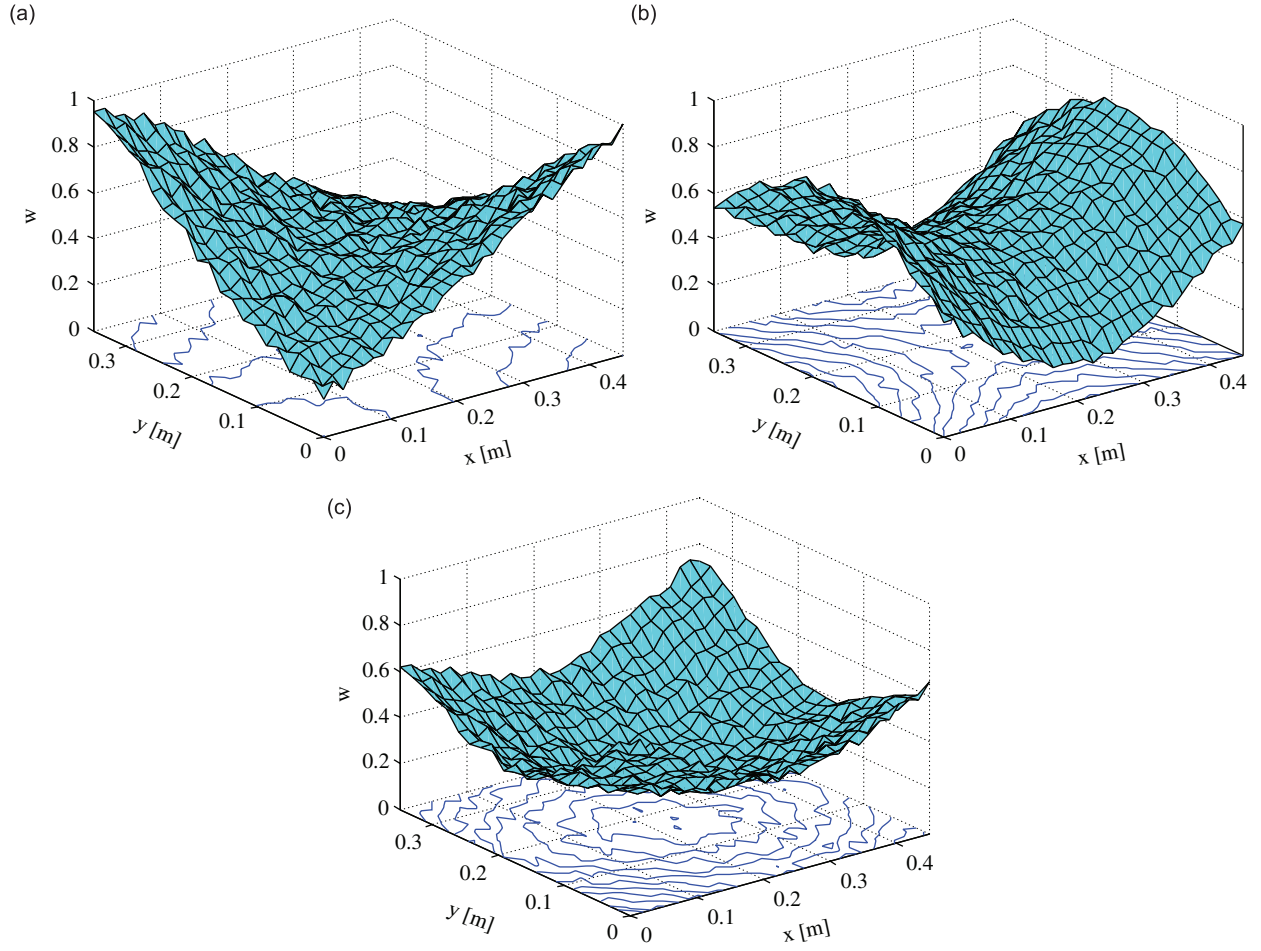

Fig. 4. Numerical modes with noise $\leqslant$15%: (a) mode shape 1, (b) mode shape 2 and (c) mode shape 3.

4.2. Results and discussion

Fig. 3 shows three numerical modes obtained by the finite element method that were used to verify the method. Fig. 4 shows the same modes with the addition of a noise with maximum amplitude $\leqslant 15\%$ of the maximum amplitude of the mode deflection. Fig. 5 shows these same modes after smoothing.

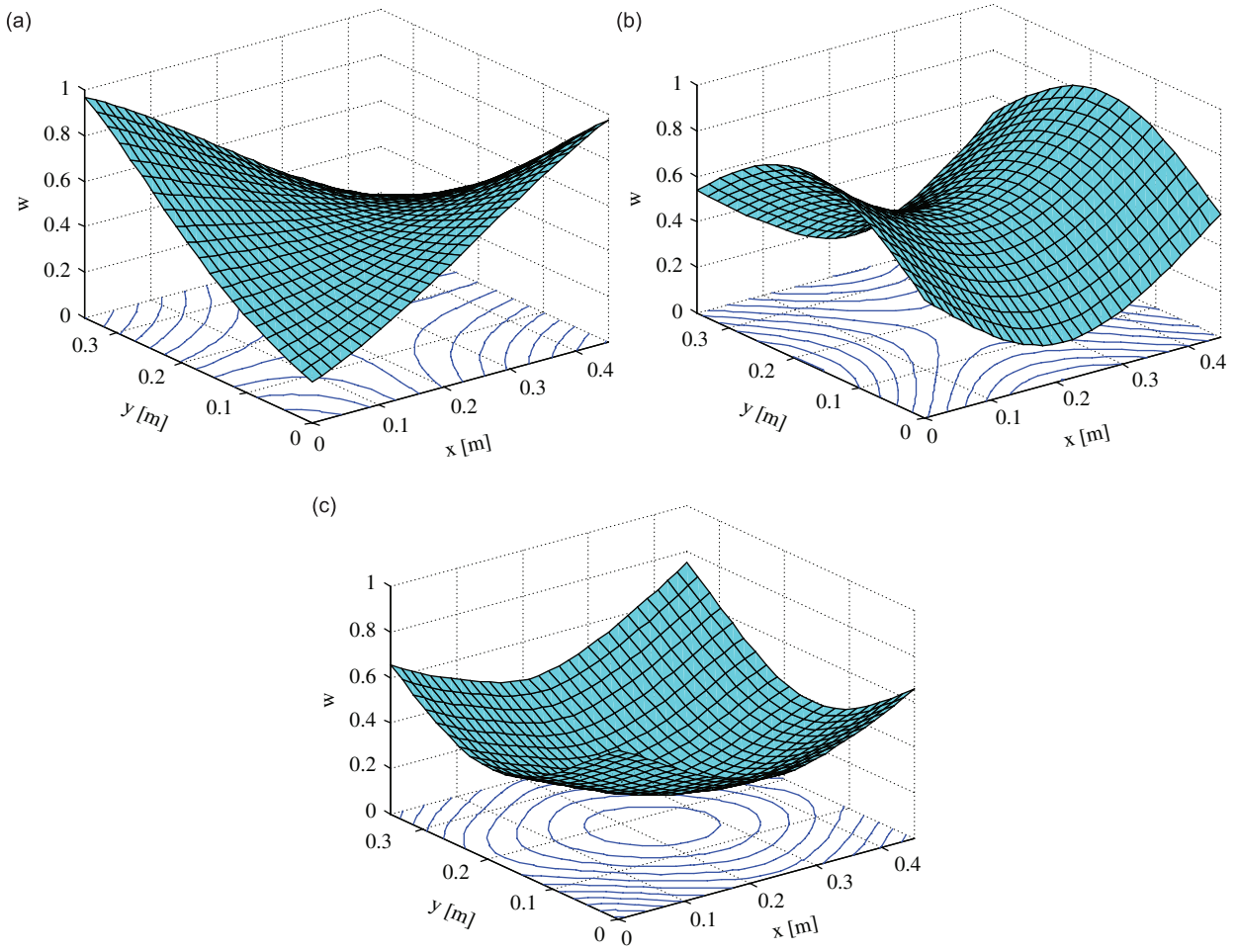

Fig. 5. Numerical modes smoothed by the RDFS: (a) mode shape 1, (b) mode shape 2 and (c) mode shape 3.

Table 2
Errors obtained using the finite differences method

Constants	Error (%)			
	Without noise	Noise $\leqslant 5\%$	Noise $\leqslant 10\%$	Noise $\leqslant 15\%$
D_{11}	0.02	1.61	2.44	2.78
D_{22}	0.04	5.77	13.274	21.46
D_{12}	0.02	16.84	29.48	38.34
D_{66}	1.22	4.55	11.05	17.59
D_{16}	0.63	3.42	9.13	16.04
D_{26}	0.64	11.72	19.59	23.31

Table 2 shows values of errors obtained for the numerical anisotropic plate in the absence of noise and in the presence of different levels of noise. The derivatives were computed by directly applying the finite difference method. As can be seen, this method is not suitable to be used in the presence of noise, because the values of elastic constants present significant errors. However, it is a very accurate method when the signal is devoid of noise. This can be explained by the fact that the computation of derivatives is extremely sensitive to noise. Therefore, if finite differences are used on a signal containing noise, the signal should be subjected to a filtering process before using this method. The RDFS can be an alternative option for filtering a noisy signal.

Table 3 shows values of the errors obtained for the numerical anisotropic plate in the absence of noise but using RDFS. For analogy to K_ξ and K_η (in Section 2.3), variables K_x and K_y represent the ratios R/M and C/N along directions x and y, respectively. The subscripts 1, 2, and 3 in the variables p, q, K_x, and K_y refer to the three used mode shapes. For this case, very high values of parameters p and q are used. As can be seen, in the

Table 3
Errors obtained after smoothing by RDFS—numerical anisotropic plate without noise

Optimum parameters: $p_1 = 8$, $p_2 = 8$, $p_3 = 8$, $q_1 = 8$, $q_2 = 8$, $q_3 = 8$ Adjusted values after smoothing: $K_{x1} = 2$, $K_{x2} = 2$, $K_{x3} = 2$, $K_{y1} = 2$, $K_{y2} = 2$, $K_{y3} = 2$ Constants	Error (%) Without noise
D_{11}	0.25
D_{22}	0.19
D_{12}	0.83
D_{66}	1.25
D_{16}	0.31
D_{26}	0.54

Table 4
Errors obtained after smoothing by RDFS—numerical anisotropic plate with noise

Optimum parameters: $p_1 = 2$, $p_2 = 1$, $p_3 = 1$, $q_1 = 1$, $q_2 = 3$, $q_3 = 4$					
Noise $\leqslant 5\%$ Adjusted values: $K_{x1} = 10.38$, $K_{x2} = 1.85$, $K_{x3} = 1.62$, $K_{y1} = 3.85$, $K_{y2} = 3.14$, $K_{y3} = 1.53$ Elapsed time: 25.475 s		Noise $\leqslant 10\%$ Adjusted values: $K_{x1} = 15.37$, $K_{x2} = 1.89$, $K_{x3} = 1.60$, $K_{y1} = 3.67$, $K_{y2} = 3.16$, $K_{y3} = 1.38$ Elapsed time: 26.436 s		Noise $\leqslant 15\%$ Adjusted values: $K_{x1} = 15.36$, $K_{x2} = 1.94$, $K_{x3} = 1.57$, $K_{y1} = 3.51$, $K_{y2} = 3.10$, $K_{y3} = 1.31$ Elapsed time: 25.532 s	
Constants	Error (%)	Constants	Error (%)	Constants	Error (%)
D_{11}	0.43	D_{11}	0.31	D_{11}	1.28
D_{22}	1.26	D_{22}	0.47	D_{22}	0.38
D_{12}	1.53	D_{12}	4.36	D_{12}	11.04
D_{66}	1.37	D_{66}	1.51	D_{66}	1.61
D_{16}	1.12	D_{16}	3.10	D_{16}	5.29
D_{26}	0.89	D_{26}	1.40	D_{26}	1.79

Table 5
Engineering constants from the used method and from the literature

Engineering constants	E_x (GPa)	E_y (GPa)	G_{xy} (GPa)	ν_{xy}
Medium values from the literature ($\rho = 7800\,\mathrm{kg/m^3}$)	210	210	80.8	0.3
Obtained values by the method ($\rho = 7870\,\mathrm{kg/m^3}$)	215.67	209.08	83.08	0.3

absence of noise, the results were as good as the results obtained without the application of the smoothing method.

Table 4 shows results obtained when noise is introduced. It can be noted that, at the same noise level, errors resulting from the direct application of finite differences are much higher than errors after pre-filtering, and the

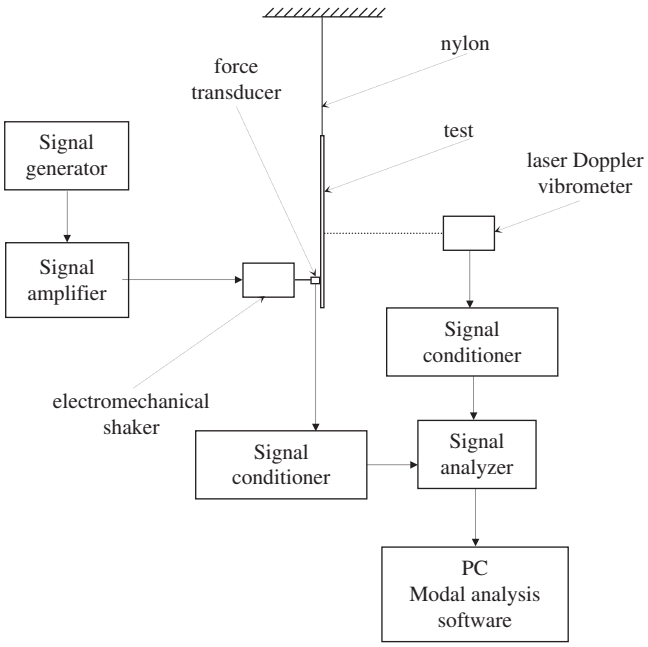

Fig. 6. Experimental setup of the modal testing.

Table 6
Comparison between experimental and numerical frequencies for the isotropic steel plate

Optimum parameters: $p_1 = 1$, $p_2 = 4$, $p_3 = 5$, $q_1 = 1$, $q_2 = 4$, $q_3 = 4$ Adjusted values after smoothing: $K_{x1} = 3.74$, $K_{x2} = 1.91$, $K_{x3} = 2.00$, $K_{y1} = 2.89$, $K_{y2} = 2.38$, $K_{y3} = 2.00$ Experimental frequencies	Numerical frequencies (ANSYS)	Differences (%)
43.09	45.27	5.07
55.95	55.07	1.58
96.61	96.72	0.11
103.97	107.67	3.56
124.61	129.18	3.67
160.37	159.79	0.36

Table 7
Comparison of experimental and numerical frequencies for the orthotropic carbon–epoxy plate

Optimum parameters: $p_1 = 2$, $p_2 = 1$, $p_3 = 2$, $q_1 = 2$, $q_2 = 4$, $q_3 = 1$ Adjusted values after smoothing: $K_{x1} = 3.90$, $K_{x2} = 1.88$, $K_{x3} = 1.91$, $K_{y1} = 2.56$, $K_{y2} = 2.08$, $K_{y3} = 1.43$ Experimental frequencies	Numerical frequencies (ANSYS)	Differences (%)
41.32	40.26	2.57
99.59	95.47	4.13
126.53	125.70	0.65
166.76	170.88	2.47
183.97	188.56	2.49
256.21	257.00	0.30

elapsed time by the whole identification process is very low, independently of the noise level. For each value of variables p and q, the ratios K_x and K_y of the RDFS were estimated from an optimization process, as proposed by Vanherzeele [17]. These ratios, which represent the design variables of the minimization problem, are highly dependent on variables p and q. When p and q increase, the residual usually decreases. However, if the original signal contains noise, it is possible that noise is not being filtered. On the other hand, if p and q decrease, the residual value increases. Depending on the curvature of the original mode, part of data of the real signal (real curvature of the mode) is filtered. In general, p and q depend on the shape of the signal. If the signal is smooth and has few wave peaks, p and q are small. On the other hand, if the signal has many wave peaks, p and q are larger. In this work, the finite element method was used to ascertain the coherence of the computed elastic properties. Parameters p and q were changed and the elastic constants computed. These constants are input data to calculate the numerical frequencies. The parameters are changed until the difference between experimental and numerical natural frequencies is minimal for the same mode shapes.

Another RDFS variable that can contribute to the accuracy of the computed elastic constants is the number of points on the mesh. Errors generally decrease as mesh discretization increases. Due to this problem, it is advisable to either increase the number of measured points in the modal analysis or create points by interpolation of the original signal before the smoothing process. This procedure is possible because this method is not very sensitive to noise, but its accuracy depends on the number spectral lines to approximate the coefficients of the Fourier series. Increasing the number of points on the mesh also contributes positively to the computation of the second-order derivatives by the finite difference method.

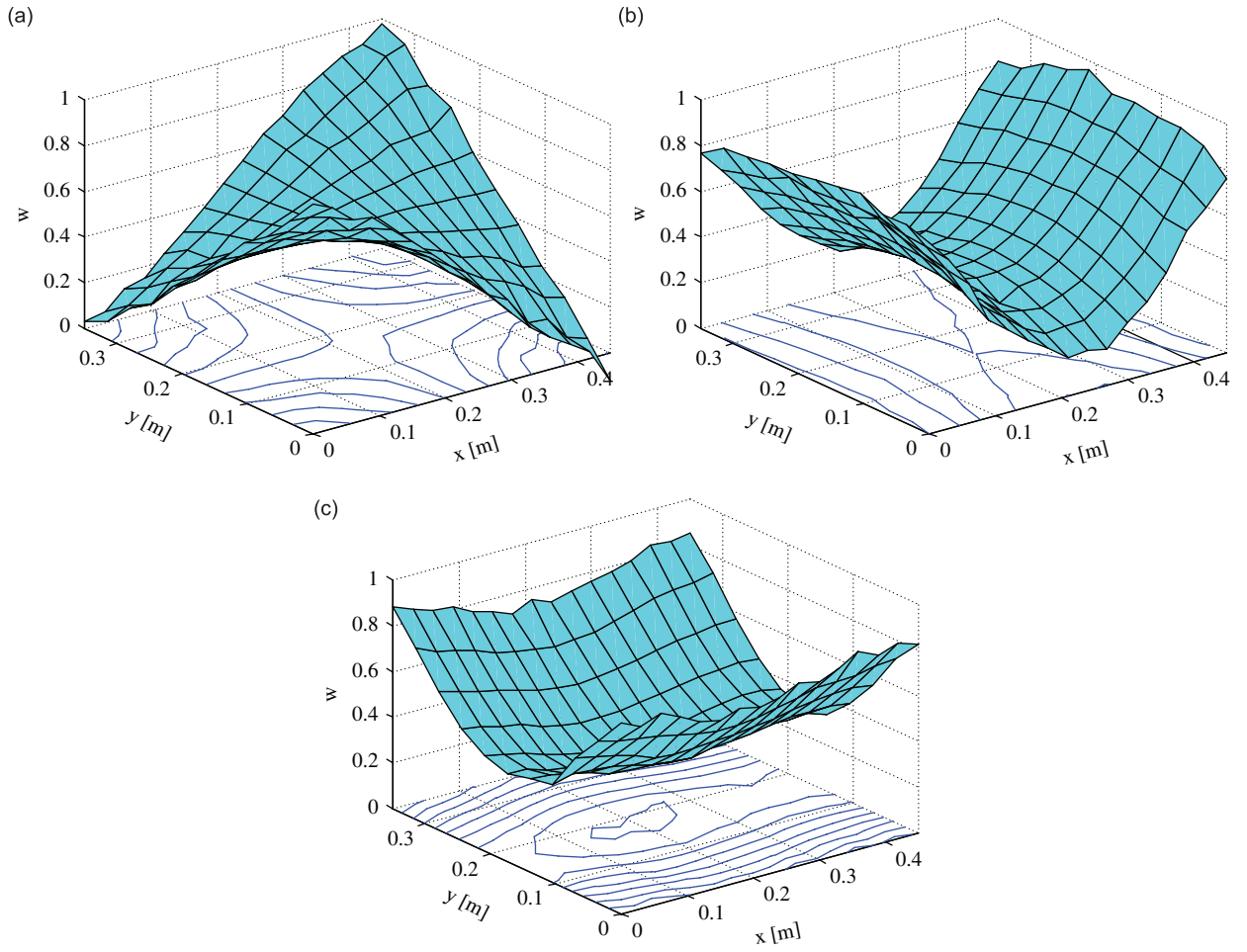

Fig. 7. Experimental modes of the steel plate: (a) mode shape 1, (b) mode shape 2 and (c) mode shape 3.

5. Experimental analysis

5.1. Presentation of experimental setup and procedures

Next, the proposed method was used with data obtained from the experimental modal analysis of two plates. One was a $450 \times 350 \times 2.1$ mm isotropic steel plate with a total measured mass of 2.603 kg. The other was a $444 \times 346 \times 3.2$ mm orthotropic carbon/epoxy plate with woven fibers with a total measured mass of 0.7594 kg. The mass densities of the plates were obtained by dividing the measured mass by the volume. For the steel plate, it was found a value that is slightly higher than the medium value found in the literature, as can be seen in Table 5. This was due to variations in the thickness along the domain of the plate. As the proposed method is sensitive to the variation of the thickness, computing the density from the measured mass instead of using values from literature can be a way to compensate for the variations of the plate thickness.

The plates were suspended by nylon strings to simulate free-edge boundary conditions, as illustrated in Fig. 6. The plates were excited at a unique point through a stinger and a force transducer by an electromechanical shaker fed with white noise. The frequency range of the input signal was chosen such that it excited the three required modes. Dynamic responses (transverse velocities) were measured at 176 equally spaced points on the plates by a laser Doppler vibrometer. Frequency response functions (FRFs) were obtained using the commercial software LMS/CADA-X®. The mode shapes were identified by ERA

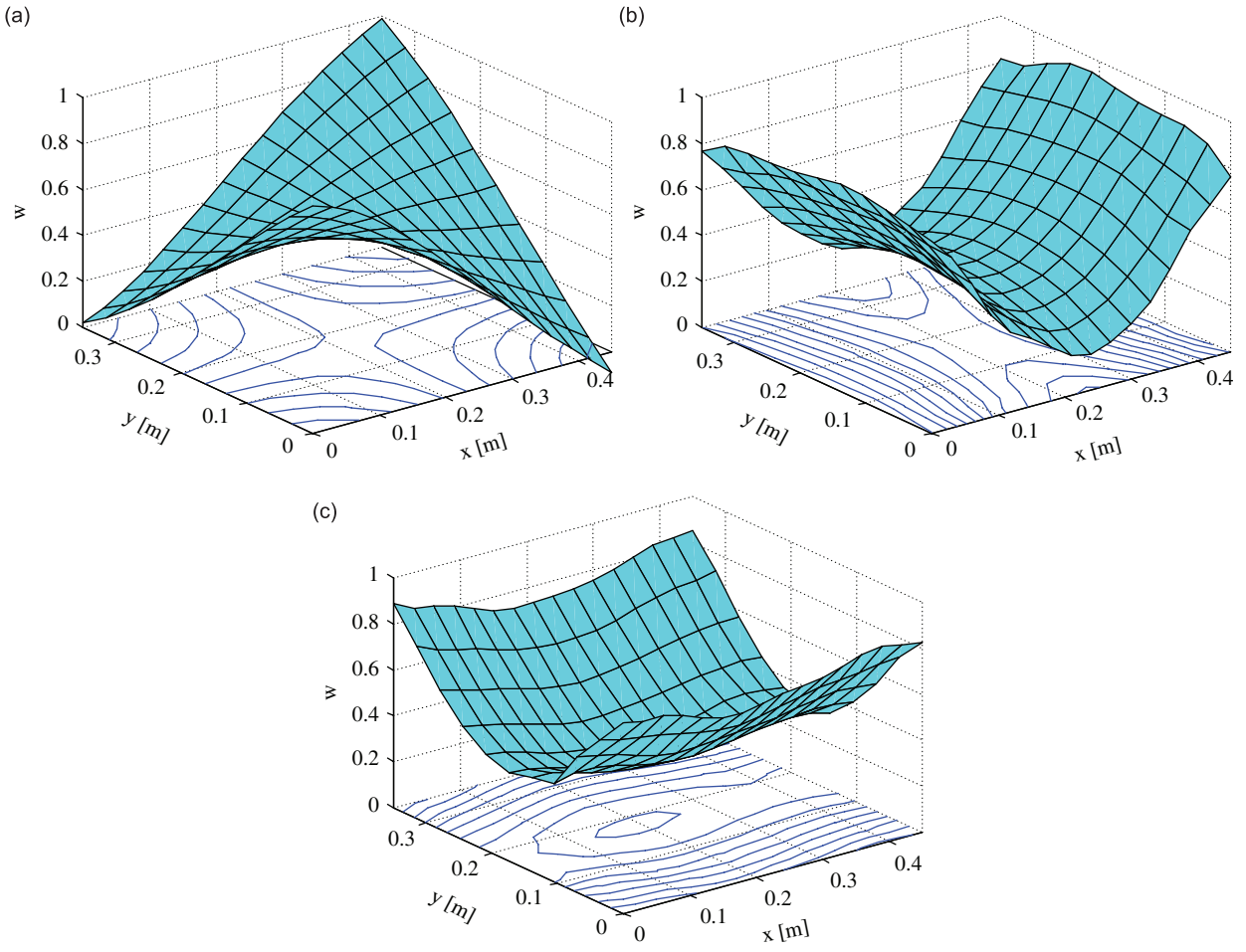

Fig. 8. Experimental modes of the steel plate smoothed by the RDFS: (a) mode shape 1, (b) mode shape 2 and (c) mode shape 3.

(Eigen System Realization Algorithm) [18] using impulse response functions (in the time domain) obtained from the measured FRFs by the inverse Fourier transform.

5.2. Results and discussion

Table 5 shows the values of the engineering constants of the steel calculated from the D_{ij} and the one from the literature, where E_x and E_y are the longitudinal modulus of elasticity associated with the x and y directions of the plate, respectively, G_{xy} is shear modulus associated with the xy plate plane, and v_{xy} is the Poisson's ratio. Tables 6 and 7 contain values of errors of numerical and experimental natural frequencies for the isotropic and orthotropic plates, respectively, using the RDFS. As can be seen, the results were satisfactory.

Figs. 7 and 9 show three modes (twisting and bending along the x and y directions) obtained by the experimental test on the isotropic steel plate and the orthotropic carbon–epoxy plate, respectively. Figs. 8 and 10 show the same modes after smoothing (Figs. 7–10).

Fig. 11(a) shows the second-order spatial derivative with respect to y of the twisting mode computed directly by finite differences, while Fig. 11(b) shows the same second derivative of the twisting mode obtained by finite differences after the smoothing process. Note that the second derivative computed directly by finite differences

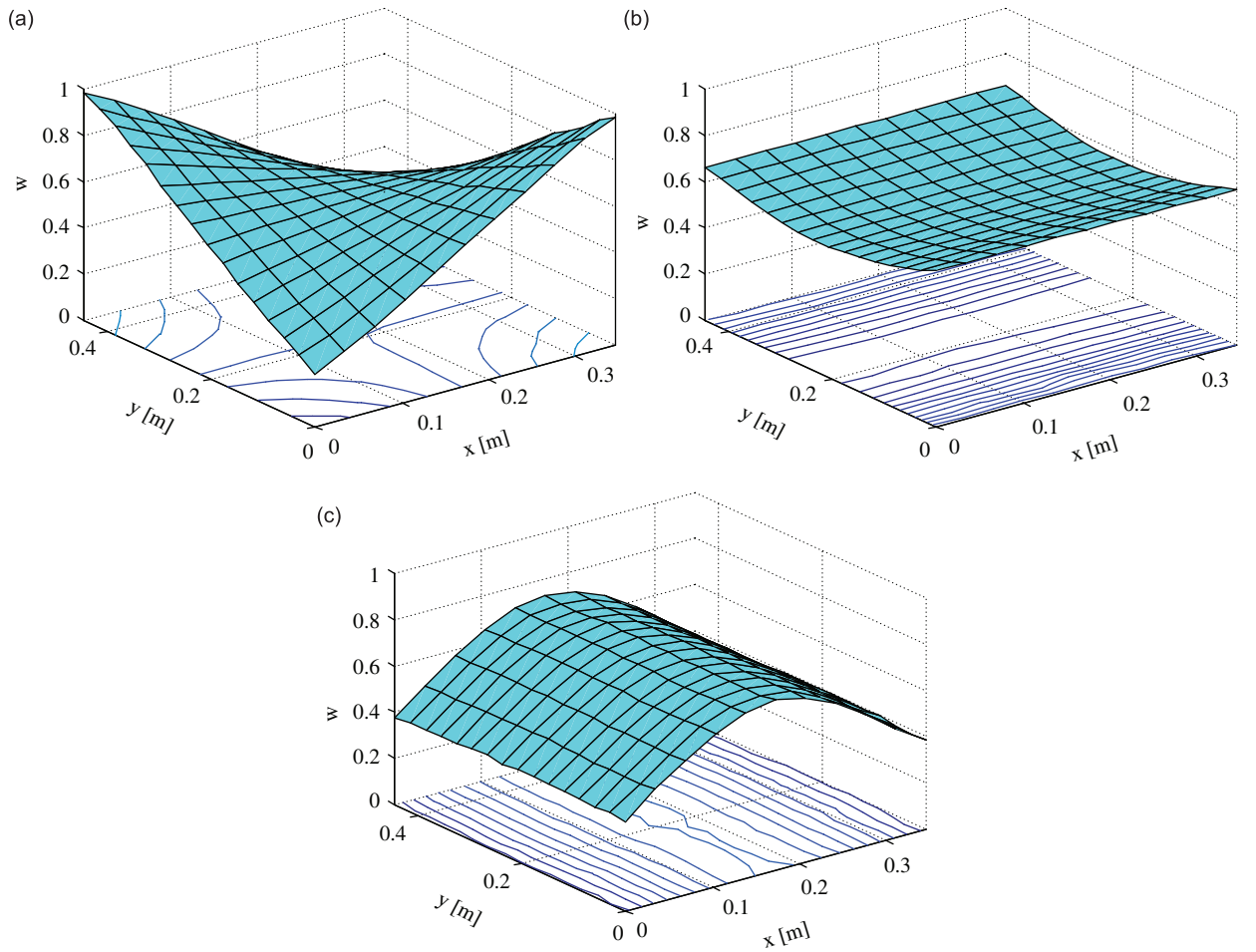

Fig. 9. Experimental modes of carbon–epoxy plate: (a) mode shape 1, (b) mode shape 2 and (c) mode shape 3.

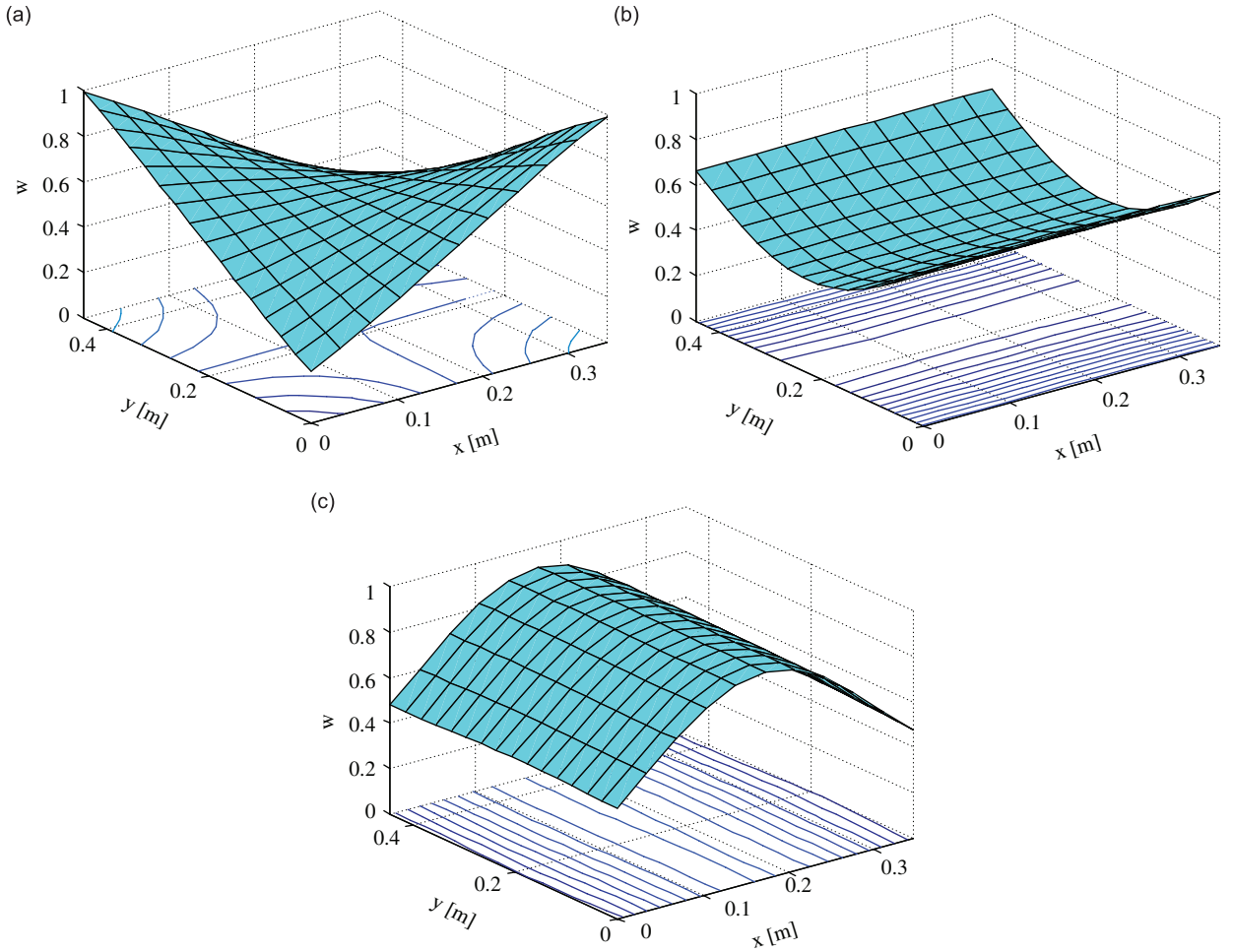

Fig. 10. Experimental modes of the carbon–epoxy plate smoothed by the RDFS: (a) mode shape 1, (b) mode shape 2 and (c) mode shape 3.

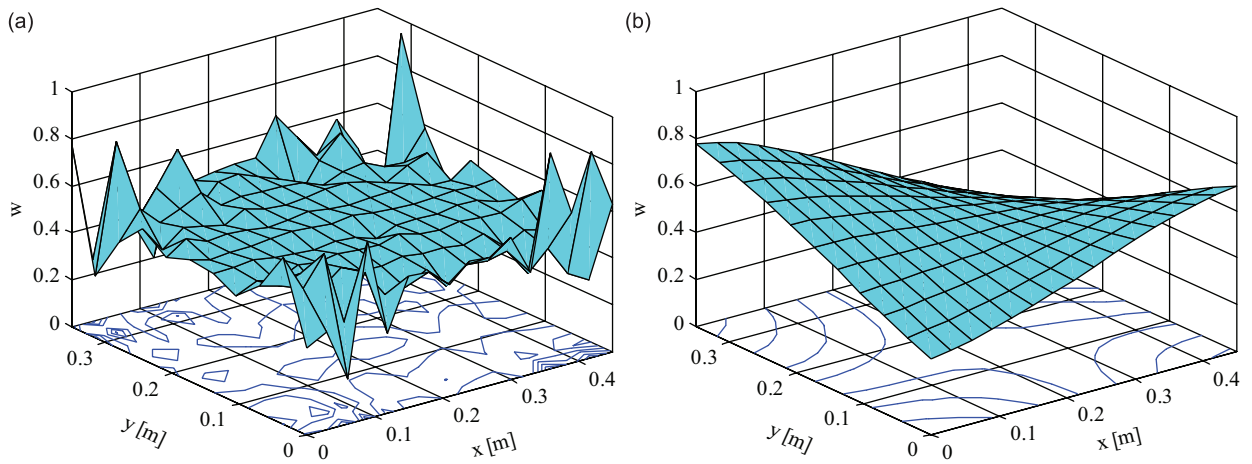

Fig. 11. Second derivative along the direction y of the twisting mode of the steel plate: (a) before smoothing process and (b) after the smoothing process using the RDFS.

is completely meaningless, because the noise derivative predominates over the signal derivative. The reduction of the noise obtained by RDFS allows the second derivative to be properly computed.

6. Conclusions

This paper presented an alternative approach to compute elastic constants directly from experimental modal analysis. No special devices were used to obtain mode shapes and a certain level of noise was allowed in the experimental data. The use of the RDFS to smooth mode shapes before computation of the second-order spatial derivatives by finite differences improved the accuracy in the identification of elastic constants. This smoothing method is very fast and proved suitable for smoothing noise-contaminated two-dimensional functions.

Acknowledgments

The authors are grateful to ALLTEC for the donation of the carbon–epoxy laminated plate, and to the Brazilian Council for Scientific and Technological Development (CNPq) and the State of São Paulo Research Foundation (FAPESP) for their financial support of this work.

References

[1] D.F. Adams, L.A. Carlsson, R.B. Pipes, *Experimental Characterization of Advanced Composite Materials*, CRC Press, Boca Raton, 2003.
[2] E.O. Ayorinde, R.F. Gibson, Improved method for in-situ elastic constants of isotropic and orthotropic composite materials using plate modal data with trimodal and hexamodal Rayleigh formulations, *Journal of Vibration and Acoustics* 117 (1995) 180–186.
[3] E.O. Ayorinde, L. Yu, On the use of diagonal modes in the elastic identification of thin plates, *Journal of Vibration and Acoustics* 121 (1999) 33–40.
[4] J.M. Berthelot, F. Anoulvant, Measuring the bending stiffness of orthotropic and symmetric laminates from flexural vibration, *Journal of Composite materials* 36 (2001).
[5] P.S. Frederiksen, Parameter uncertainty and design of optimal experiments for estimation of elastic constants, *International Journal of Solids and Structures* 35 (1998) 1241–1260.
[6] R.F. Gibson, Modal vibration response measurements for characterization of composite materials and structures, *Composites Science and Technology* 60 (2000) 2769–2780.
[7] K. Hosokawa, K. Matsumoto, Identification of elastic parameters for laminate circular cylindrical shells (comparison of numerical and experimental results), *JSME International Journal Series C* 45 (1) (2002).
[8] F.B. Batista, E.L. Albuquerque, M. Dias Jr., Determination of elastic constant on thin plates of composite materials using numerical methods, modal analysis, and optimization, *XXVI Iberian Latin–American Congress on Computational Methods in Engineering* (*CILAMCE*), Guarapari, 2005 (in Portuguese).
[9] F.B. Batista, Identification of Elastic Parameters on Thin Plates of Composite Materials, Master Thesis, State University of Campinas, 2005.
[10] T. Lauwagie, H. Sol, W. Heylen, G. Roebben, Determination of in-plane elastic properties of the different layers of laminated plates by means of vibration testing and model updating, *Journal of Sound and Vibration* 274 (2004) 529–546.
[11] R. Rikards, A. Chate, G. Gailis, Identification of elastic properties of laminates based on experiment design, *International Journal of Solids and Structures* 38 (2001) 5097–5115.
[12] S. Hwang, C. Chang, Determination of elastic constants of materials by vibration testing, *Composite Structures* 49 (2000) 183–190.
[13] M. Grédiac, P.A. Paris, Direct identification of elastic constants of anisotropic plates by modal analysis, *Journal of Sound and Vibration* 195 (1996) 401–415.
[14] M. Grédiac, N. Founier, P.A. Paris, Y. Surrel, Direct identification of elastic constants of anisotropic plates by modal analysis: experimental results, *Journal of Sound and Vibration* 210 (1998) 643–659.
[15] A. Giraudeau, F. Pierron, Identification of stiffness and damping properties of thin isotropic vibration plates the virtual fields method theory and simulations, *Journal of Sound and Vibration* 284 (2005) 757–781.
[16] J.R.F. Arruda, Surface smoothing and partial spatial derivatives computation using a regressive discrete Fourier series, *Mechanical Systems and Signal Processing* 6 (1992) 41–50.
[17] J. Vanherzeele, Design of Regressive Fourier Techniques for Processing Optical Measurements, PhD Thesis, Vrije Universiteit Brussel, 2007.
[18] J. Juang, *Applied System Identification*, Facsimile ed., Prentice Hall PTR, Englewood Cliffs, NJ, 1993.